Research Paper https://doi.org/10.7733/jnfcwt.2020.18.3.355

Corrosion Behavior of Inconel X-750 for Carbon Anode Oxide Reduction Application

Min Ku Jeon[1,2,*], Sung-Wook Kim[1], Sang-Kwon Lee[1], and Eun-Young Choi[1,2]
[1]*Korea Atomic Energy Research Institute, 111, Daedeok-daero 989beon-gil, Yuseong-gu, Daejeon, Republic of Korea*
[2]*University of Science and Technology, 217, Gajeong-ro, Yuseong-gu, Daejeon, Republic of Korea*

(Received April 21, 2020 / Revised June 12, 2020 / Approved July 20, 2020)

The corrosion behavior of the Inconel X-750 alloy was investigated for its potential application under a Cl_2-O_2 mixed gas flow in an Ar atmosphere. The corrosion rate was found to be negligible at temperatures up to 400℃ under a flow rate of 30 mL·min^{-1} Cl_2 + 170 mL·min^{-1} Ar, whereas an exponential increase was observed in the corrosion rate at temperatures greater than 500℃. The suppression of the corrosion reaction due to the presence of O_2 was verified experimentally at flow rates of 30 mL·min^{-1} Cl_2 (4.96 g·m^{-2}·h^{-1}), 20 mL·min^{-1} Cl_2 + 10 mL·min^{-1} O_2 (2.02 g·m^{-2}·h^{-1}), and 10 mL·min^{-1} Cl_2 + 20 mL·min^{-1} O_2 (1.34 g·m^{-2}·h^{-1}) under a constant Ar flow rate of 170 mL·min^{-1} at 600℃ for 8 h. The surface morphology analysis results revealed that porous surfaces with tunnel-type holes were produced under the Cl_2-O_2 mixed-gas condition. Furthermore, the effects of the Cl_2 flow rate on the corrosion rate were investigated, indicating that its impact was negligible within the range of 5–30 mL·min^{-1} Cl_2 at 600℃.

Keywords: : Inconel X-750, Chlorine, Oxygen-chlorine mixed gas, Oxide reduction, Pyroprocessing

*Corresponding Author.
Min Ku Jeon, Korea Atomic Energy Research Institute, E-mail: minku@kaeri.re.kr, Tel: +82-42-868-2435

ORCID

Min Ku Jeon	http://orcid.org/0000-0001-8115-3241	Sung-Wook Kim	http://orcid.org/0000-0002-5537-4793
Sang-Kwon Lee	http://orcid.org/0000-0003-4118-5024	Eun-Young Choi	http://orcid.org/0000-0003-1693-7642

1. Introduction

The oxide reduction (OR) process enables the use of used oxide fuel discharged from light water reactors in the electrochemical pyroprocessing which was initially designed for metal fuels in the Experimental Breeder Reactor-II (EBR-II) project [1]. There are two explanations of possible OR process mechanisms. One is a direct electrochemical reduction mechanism, which can be expressed with the following reaction equation, which operates at 2.40 V.

$UO_2 \rightarrow U + O_2$ (g)
(Forward reaction ΔG = 925 kJ at 650℃)

The second mechanism is a chemical reduction mechanism, which suggests that Li_2O dissolved in LiCl salt is decomposed to produce metallic Li and oxygen gas at 2.47 V. The metallic Li produced at the cathode reacts with UO_2 according to the following reaction equations.

$Li_2O \rightarrow 2\ Li + 1/2\ O_2$ (g)
(Electrochemical, forward reaction ΔG = 477 kJ at 650℃)

$UO_2 + 4\ Li$ (l) $\rightarrow U + 2\ Li_2O$
(Chemical, forward reaction ΔG = -26.8 kJ at 650℃)

Either way, a noble metal electrode (normally Pt) is employed as the anode material to produce oxygen gas at the operating condition of 650℃ [2-5]. The use of Pt limits the maximum potential applicable to the cell due to the associated dissolution reaction, and degradation of a Pt electrode via repeated OR operations was recently documented [6]. Previously, carbon was proposed as an alternative to expensive Pt; however, the formation of carbonate ions (CO_3^{2-}) and their decomposition product, carbon dust, was indicated as a key issue that prevented the use of carbon in the OR process [7].

Recently, the carbon anode was revisited by our group for use in the OR process at a high anode potential to solve abovementioned Pt and carbonate issues [8, 9]. High-potential operation employs the following electrochemical reaction in order to produce metallic Li, which can reduce UO_2 into U, as noted above.

$LiCl$ (l) $\rightarrow Li$ (l) $+ 1/2\ Cl_2$ (g)
(Forward reaction ΔG = 368 kJ at 650℃)

This reaction occurs at 3.81 V according to the Gibbs free energy of the reaction. It was experimentally shown that this approach could suppress the accumulation of carbonate ions, presumably owing to the reaction with chlorine gas near the anode [8, 9]. These operations were demonstrated at around 10~15 V, which is several times higher than the level of 3~3.4 V in the Pt case. Although the high-potential carbon anode has brought profound advantages for OR operations, a new problem also arose: chlorine [9]. It is well known that chlorine is a corrosive gas, especially at high temperatures. Severe corrosion of equipment components after several operations of the high-potential carbon anode OR was observed in our previous work [9].

The gas stream predicted during OR operation with the high-potential carbon anode is a mixture of Cl_2, O_2, CO, CO_2, and Ar. Here, argon is an atmospheric gas in the OR operation environment. Among these gases, we focused on the impact of chlorine and oxygen against corrosion of the equipment, as corrosion by the other gases is likely low. The corrosion behavior of certain commercial alloys under a Cl_2 or HCl atmosphere was previously investigated, and it was shown that pure nickel and its alloys, specifically Inconel and Hastelloy, had much lower corrosion rates than those of carbon steels [10]. The corrosion behaviors of iron [11], nickel [12], and chromium [13] in an HCl-O_2 mixed atmosphere were investigated by Ihara et al. However, the corrosion behavior of commercial metals under a Cl_2-O_2 mixed atmosphere is not available. As a starting point, our group investigated the corrosion behavior of stainless steel 316 (SS-316) under a Cl_2-O_2 mixed atmosphere [14]. Interestingly, it was found that the presence of oxygen

significantly reduced the chlorine-induced corrosion rate of SS-316. However, the exponential increase in the corrosion rate with an increase in the reaction temperature suggested limited application of SS-316 at or below 300℃ under a chlorine atmosphere. In the present study, Inconel X-750 was employed to verify its applicability to high-potential carbon anode OR equipment. The effects of the reaction temperature, Cl_2-O_2 composition, and Cl_2 flow rate were investigated.

2. Experimental

A quartz tube (40 mm diameter) was employed as the corrosion reactor in this study. The tube was positioned horizontally and the middle part was heated using an electrical furnace (equipped with Kanthal A-1 heating element along 120 mm length of heating zone). One end of the quartz tube was connected to three mass flow controllers (MFCs), while the other end was connected to a dry Cl_2 scrubbing system which was designed to adsorb residual Cl_2 gas in the exhaust gas stream. Schematic diagram of the experimental set-up can be found in our previous work [14].

An Inconel X-750 plate (purchased from Nilaco co., Japan, 1.0 mm thickness with major constituents of Ni (~70%), Cr (14~17%), Fe (5~9%), and Ti (2.25~2.75%)) was cut into 30 mm × 10 mm pieces and four of them were utilized in every experiment. The specimens were thoroughly washed with deionized (DI) water and ethanol (Daejung chemicals and metals co., Korea, anhydrous ethanol, 99.9%) before the corrosion experiments. The average weight of the samples (four pieces) was 10.172 g. The flow rates of the feed gases were individually controlled using MFCs (purchased from Kofloc co., Japan) for each gas (Model 5400 for Cl_2 and Model 3660 for Ar and O_2). It should be noted that the specimens were not polished in order to mimic the actual manufacturing condition of OR equipment, including a native oxide layer.

The effect of the corrosion reaction temperature was investigated in a temperature range of 300~700℃ by flowing

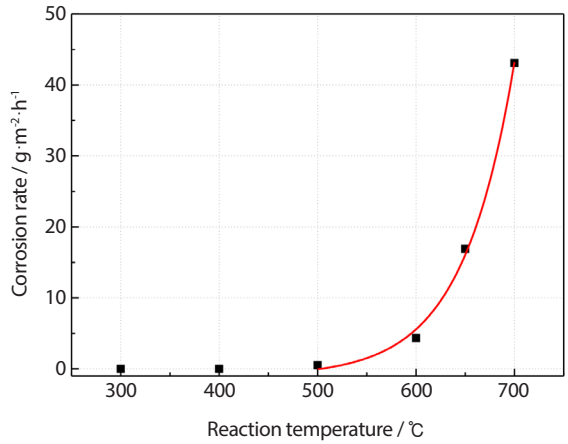

Fig. 1. Corrosion rate of Inconel X-750 as a function of the reaction temperature. Experiments were conducted for 8 h under a 30 mL·min^{-1} Cl_2 + 170 mL·min^{-1} Ar flow. Fitting result is also included in the range of 500~700℃.

170 mL·min^{-1} Ar + 30 mL·min^{-1} Cl_2 for 8 h. The effect of the mixed gas feed was identified by flowing various gas compositions of 30 mL·min^{-1} Cl_2, 20 mL·min^{-1} Cl_2 + 10 mL·min^{-1} O_2, and 10 mL·min^{-1} Cl_2 + 20 mL·min^{-1} O_2 at 600℃ while the flow rate of Ar was kept constant at 170 mL·min^{-1}. During the mixed gas effect experiments, tests were conducted for various reaction durations of 2, 4, 8, and 16 h. Additional experiments were performed for various chlorine flow rates of 5, 10, and 20 mL·min^{-1} at 600℃ with an argon balance flow for a total flow rate of 200 mL·min^{-1} without oxygen. After each experiment, the samples were washed using DI water and ethanol to remove any adhering chlorides or oxides.

The effect of the gas compositions on the surface morphology was investigated using a scanning electron microscopy (SEM, Hitachi SU-8020) system with energy dispersive spectroscopy (EDS) for a composition analysis.

3. Results and discussion

The effect of the reaction temperature under a Cl_2–Ar flow condition was investigated, and these results are shown in Fig. 1. It should be noted that the corrosion rate was

negligible at 300 and 400℃, meaning that the weight change was less than 1 mg (= 0.00983%). Beginning at 500℃, the corrosion rate increased exponentially with an increase in the reaction temperature. The corrosion rate measured at 500℃ was 5.01×10^{-1} g·m^{-2}·h^{-1}, which is far below the rate of 1.98×10^{1} g·m^{-2}·h^{-1} for SS-316 at 500℃ [14]. Although Inconel X-750 proved its superior resistance against chlorine gas, the corrosion rate increases too rapidly to be employed at or above 600℃. These results are in agreement with those in previous work that suggested an operation temperature of 538℃ for Inconel and Hastelloy alloys under a Cl_2 atmosphere [10]. The exponential relationship between the reaction temperature (in *K*) and the corrosion rate is displayed in Fig. 1. The following equation was achieved from the fitting result:

$$\text{Corrosion rate (g·m}^{-2}\text{·h}^{-1}) = (4.092 \times 10^{-7})\, e^{(T\,(K)/52.60)} - 1.042 \quad (1)$$

It is important to note that this corrosion rate equation is applicable only to the experimental condition in this study.

After the corrosion experiment at 700℃, a significant amount of yellowish corrosion product was observed in both the residual specimens and the end part of the quartz tube, as shown in Fig. 2. The residual specimens were covered by dense dark brown layers with thin yellow flakes. The corrosion products were easily removed by washing to expose the metallic surface, as shown in the figure (After washing). An image of the evaporated corrosion product is also shown in Fig. 2 (Evaporated product); it is composed of yellowish and brown particles which appear similar to those covering the residual specimen. Although the major constituents of Inconel X-750 are Ni (~ 70%), Cr (14~17%), Fe (5~9%), and Ti (2.25~2.75%), only Ni and Cl were detected in the EDS analysis result of the evaporated corrosion product.

The effects of the gas composition and reaction time on the weight change of specimens are shown in Fig. 3. In the 30 mL·min^{-1} Cl_2 case (Fig. 3(a)), a weight increase

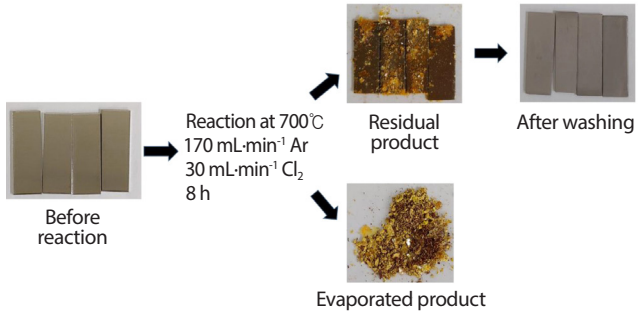

Fig. 2. Images of Inconel X-750 specimens before and after the corrosion test at 700℃ under a 30 mL·min^{-1} Cl_2 + 170 mL·min^{-1} Ar flow for 8 h.

was observed at reaction times of 2 and 4 h owing to the formation of chloride scale and the relatively slow evaporation of the scale. With an increase in the reaction time, the gap between the findings before and after washing becomes larger, suggesting that the formation rate of chloride scale is faster than its evaporation rate under the 30 mL·min^{-1} Cl_2 + 170 mL·min^{-1} Ar condition. In the presence of oxygen, the weight decrease was significantly reduced in both the 20 mL·min^{-1} Cl_2 + 10 mL·min^{-1} O_2 and 10 mL·min^{-1} Cl_2 + 20 mL·min^{-1} O_2 cases (Fig. 3(b) and 3(c), respectively). It is interesting to observe that the gap between the outcomes before and after washing decreases with an increase in the ratio of oxygen. This result suggests that the formation rate of chlorides is suppressed by oxygen, while the impact is relatively low against the evaporation rate. A comparison graph is drawn in Fig. 3(d), and it is clear that the presence of oxygen significantly suppressed the corrosion reaction. However, it needs to note that the effect of oxygen flow rate was subtle. The changes in the corrosion rate with the reaction time and gas composition are summarized in Fig. 3(e). Again, it is clear that the presence of oxygen profoundly reduces the corrosion rate, while the impact of oxygen flow rate is relatively low. A comparison experiment carried out by flowing 20 mL·min^{-1} Cl_2 + 180 mL·min^{-1} Ar clearly proved the impact of oxygen, as shown in the figure. It is also important to note that the corrosion rate decreased with an increase in the reaction time, especially in the 30 mL·min^{-1} Cl_2 + 170 mL·min^{-1} Ar case. The formation and

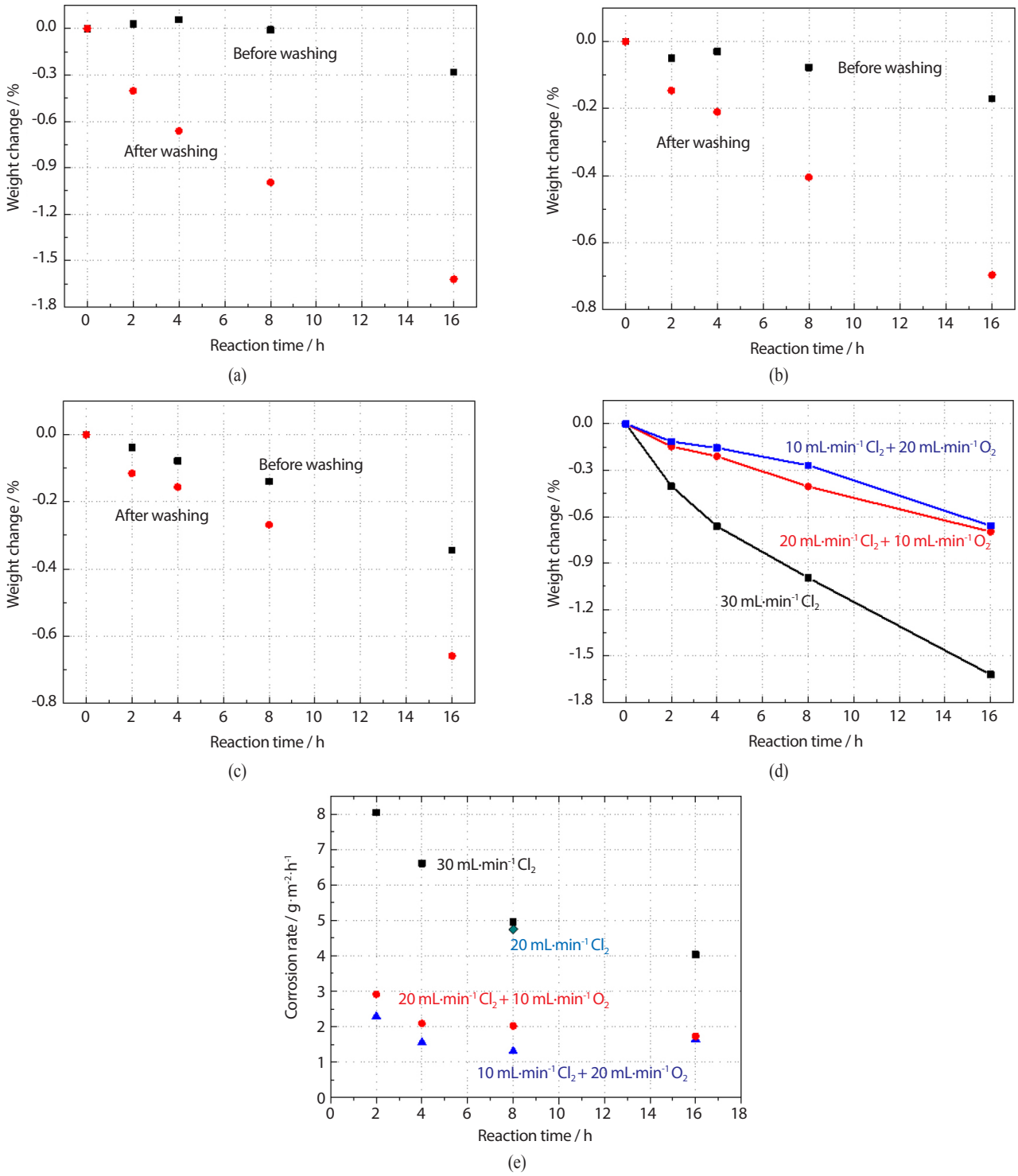

Fig. 3. Weight change measurement results after the corrosion experiments at 600℃ for various reaction durations with flow rates of (a) 30 mL·min^{-1} Cl_2 + 170 mL·min^{-1} Ar, (b) 20 mL·min^{-1} Cl_2 + 10 mL·min^{-1} O_2 + 170 mL·min^{-1} Ar, and (c) 10 mL·min^{-1} Cl_2 + 20 mL·min^{-1} O_2 + 170 mL·min^{-1} Ar. (d) Summary of the after-washing weight change results as a function of the Cl_2-O_2 composition. (e) Summary of the corrosion rates as a function of the Cl_2-O_2 composition and the reaction time. The result when flowing 20 mL·min^{-1} Cl_2 + 180 mL·min^{-1} Ar is also included.

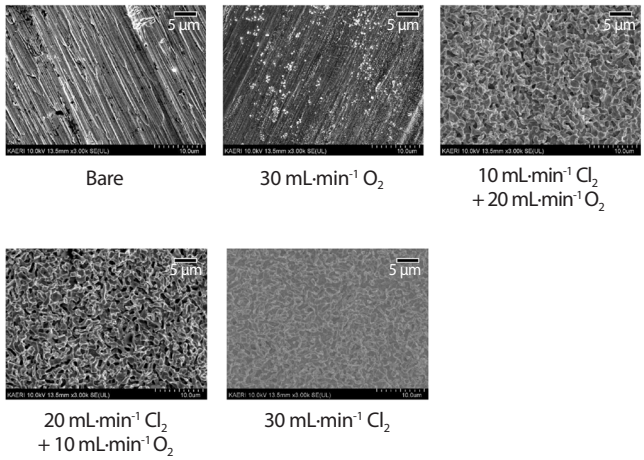

Fig. 4. SEM images after the corrosion tests at 600℃ for 16 h under various Cl_2-O_2 flow rates.

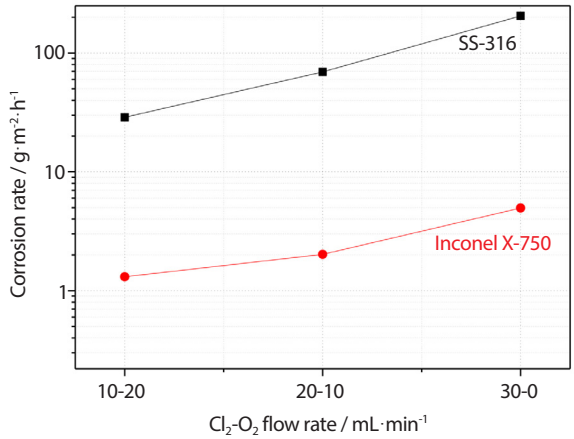

Fig. 5. Comparison of the corrosion rates between Inconel X-750 and SS-316 as a function of the Cl_2-O_2 flow rate measured after reaction at 600℃ for 8 h.

relatively slow evaporation rate of chloride scale as discussed above may explain why the corrosion rate diminished with an increase in the reaction time. On the other hand, the effect of the reaction time on the corrosion rate was lessened in the chlorine-oxygen mixed experiments.

The SEM images shown in Fig. 4 were taken to determine the effect of the Cl_2-O_2 composition on the surface morphologies. In the 30 mL·min^{-1} Cl_2 + 170 mL·min^{-1} Ar case, a dense surface with clearly distinguishable grain boundaries is shown. Significant changes were not observed in the 30 mL·min^{-1} O_2 + 170 mL·min^{-1} Ar case except the appearance of shiny spots originated from the formation of oxide grains on the surface. A totally different story was found in the Cl_2-O_2 mixed gas cases, where the formation of porous surfaces with tunnel-type holes with diameters of approximately 1 μm was noted. This result is quite different from that with SS-316, where the formation of round pits with diameters of several hundred micrometers was observed [14]. These results suggest that the corrosion reaction with chlorine occurs via different mechanisms in Inconel X-750 and SS-316 in the presence of oxygen. However, one thing clear in Fig. 4 is that the presence of oxygen leads the chlorination reaction along the vertical direction to produce porous surfaces. However, additional investigations are necessary to determine in a crystal clear manner how oxygen works to suppress the corrosion reactions in both alloys and to determine the corrosion mechanism that leads to different surface morphologies.

The protective role of oxygen was also observed in our previous work with SS-316 [14], and a comparison chart is shown in Fig. 5. It is clear in the figure that SS-316 exhibits significantly higher corrosion rates regardless of the Cl_2-O_2 composition used. The difference in the corrosion rate increased with the chlorine flow rate from 22 (10 mL·min^{-1} Cl_2 + 20 mL·min^{-1} O_2) and 34 (20 mL·min^{-1} Cl_2 + 10 mL·min^{-1} O_2) to 41 times (30 mL·min^{-1} Cl_2). This result verifies that Inconel X-750 is a far better option for a high-potential carbon anode OR application than SS-316, though the relatively high price of Inconel X-750 should also be considered during the design of actual equipment.

Recalling that the corrosion rate in 30 mL·min^{-1} Cl_2 + 170 mL·min^{-1} Ar was very close to the outcome in the 20 mL·min^{-1} Cl_2 + 180 mL·min^{-1} Ar case, as shown in Fig. 3(e), the effect of the chlorine flow rate without oxygen became questionable. Experiments were conducted with various chlorine flow rates of 5, 10, 20, and 30 mL·min^{-1} with an argon balance flow to keep the total flow rate at 200 mL·min^{-1} without oxygen. These results are shown in

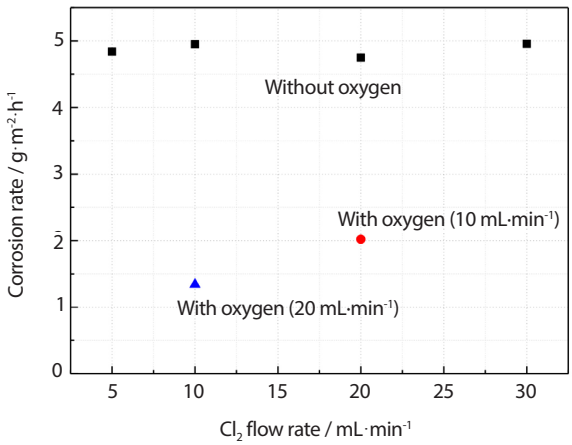

Fig. 6. Effects of the chlorine flow rate on the corrosion rate measured in a reaction at 600℃ with chlorine flow rates of 5, 10, 20, and 30 mL·min^{-1} for 8 h. The argon flow rate was controlled in each experiment to hold the total gas flow rate at 200 mL·min^{-1}.

Fig. 6, and it is obvious that the Cl_2 flow rate has no impact on the corrosion rate given the conditions used here. This result implies that the amount of chlorine generated during OR operation with the high-potential carbon anode can be neglected during equipment design efforts, whereas the impact of low concentrations of chlorine gas should not be underestimated.

4. Conclusions

Under a chlorine atmosphere, Inconel X-750 was resistant to corrosion up to 400℃, while an exponential increase in the corrosion rate was observed at temperatures greater than 500℃. The presence of oxygen significantly reduced the corrosion rate and produced porous surfaces. The corrosion rates of Inconel X-750 were only 1/22~1/41 of those of SS-316 at 600℃. The effect of the chlorine flow rate was found to be negligible in the range of 5~30 mL·min^{-1} Cl_2. Overall, Inconel is a good candidate as a high-potential carbon anode OR equipment material, although its lifetime should be considered when using it at or above 500℃ with chlorine gas.

Acknowledgement

This work was sponsored by the Nuclear R&D program of the Korean Ministry of Science and ICT (2017M2A8501 5077).

REFERENCES

[1] C.E. Stevenson, The EBR-II fuel cycle story, American Nuclear Society, La Grange Park, Illinois (1987).

[2] M. Gonzalez, A. Burak, M.F. Simpson, and S. Guo, "Identification, measurement, and mitigation of key impurities in LiCl-Li_2O used for direct electrolytic reduction of UO_2", J. Nucl. Mater., 510, 513-523 (2018).

[3] E.-Y. Choi, J. Lee, D.H. Heo, S.K. Lee, M.K. Jeon, S.S. Hong, S.-W. Kim, H.W. Kang, S.-C. Jeon, and J.-M. Hur, "Electrolytic reduction runs of 0.6 kg scale-simulated oxide fuel in a Li_2O-LiCl molten salt using metal anode shrouds", J. Nucl. Mater., 489, 1-8 (2017).

[4] S.D. Herrmann and S.X. Li, "Separation and recovery of uranium metal from spent light water reactor fuel via electrolytic reduction and electrorefining", Nucl. Technol., 171(3), 247-265 (2010).

[5] Y. Sakamura and T. Omori, "Electrolytic reduction and electrorefining of uranium to develop pyrochemical reprocessing of oxide fuels", Nucl. Technol., 171(3), 266-275 (2010).

[6] S.-K. Lee, M.K. Jeon, S.-W. Kim, E.-Y. Choi. J. Lee, S.-S. Hong, S.-C. Oh, and J.-M. Hur, "Evaluation of Pt anode stability in repeated electrochemical oxide reduction reactions for pyroprocessing", J. Radioanal. Nucl. Chem., 316(3), 1053-1058 (2018).

[7] J.-M. Hur, J.-S. Cha, and E.-Y. Choi, "Can carbon be an anode for electrochemical reduction in a LiCl-Li_2O molten salt?", ECS Electrochem. Lett., 3(10), E5-E7 (2014).

[8] S.-W. Kim, M.K. Jeon, H.W. Kang, S.K. Lee, E.-Y. Choi, W. Park, S.-S. Hong, S.-C. Oh, and J.-M. Hur,

"Carbon anode with repeatable use of LiCl molten salt for electrolytic reduction in pyroprocessing", J. Radioanal. Nucl. Chem., 310(1), 463-467 (2016).

[9] S.-W. Kim, D.H. Heo, S.K. Lee, M.K. Jeon, W. Park, J.-M. Hur, S.-S. Hong, S.-C. Oh, and E.-Y. Choi, "A preliminary study of pilot-scale electrolytic reduction of UO_2 using a graphite anode", Nucl. Eng. Technol., 49(7), 1451-1456 (2017).

[10] M.H. Brown, W.B. Delong, and J.R. Auld, "Corrosion by chlorine and by hydrogen chloride at high temperatures", Ind. Eng. Chem., 39(7), 839-844 (1947).

[11] Y. Ihara, H. Ohgame, and K. Sakiyama, "The corrosion behaviour of iron in hydrogen chloride gas and gas mixtures of hydrogen chloride and oxygen at high temperatures", Corros. Sci., 21(12), 805-817 (1981).

[12] Y. Ihara, H. Ohgame, K. Sakiyama, and K. Hashimoto, "The corrosion behaviour of nickel in hydrogen chloride gas and gas mixtures of hydrogen chloride and oxygen at high temperatures", Corros. Sci., 22(10), 901-912 (1982).

[13] Y. Ihara, H. Ohgame, K. Sakiyama, and K. Hashimoto, "The corrosion behaviour of chromium in hydrogen chloride gas and gas mixtures of hydrogen chloride and oxygen at high temperatures", Corros. Sci., 23(2), 167-181 (1983).

[14] M.K. Jeon, S.-W. Kim, and E.-Y. Choi, "Corrosion behavior of stainless steel 316 for carbon anode oxide reduction application", J. Nucl. Fuel Cycle Waste Technol., 18(2), 169-177 (2020).